Chemisorption of antimony on GaAs(110)

W. G. Schmidt, B. Wenzien, and F. Bechstedt
Friedrich-Schiller-Universität, Institut für Festkörpertheorie und Theoretische Optik, Max-Wien-Platz 1, D-07743 Jena, Germany
(Received 29 July 1993)

We report results obtained by a systematic study of Sb chemisorption on the relaxed GaAs(110) surface, using density-functional theory within the local-density approximation and norm-conserving, fully separable, *ab initio* pseudopotentials. The GaAs(110) surface is simulated by a slab geometry wherein the atomic structure of the Sb atoms at the preferred adsorption positions and the top three substrate layers is optimized by minimizing the total energy. Sb coverages of $\Theta=\frac{1}{2}$ and $\Theta=1$ are considered, corresponding to one or two Sb atoms per surface unit cell, on the average. We study nine different bonding configurations in detail. The results are interpreted in terms of the strong adsorbate-substrate bonds and the Sb-Sb interaction. For the energetically favored epitaxial continued layer structure in the $\Theta=1$ case, the atomic positions are found in good agreement with results of low-energy electron diffraction and x-ray standing wave analyses. However, the epitaxial on top structure, which seems to fit somewhat better to the scanning tunneling microscopy (STM) data, is some tenths of an eV higher in energy. In the $\Theta=\frac{1}{2}$ case we give a detailed analysis of the total-energy surface of the Sb/GaAs(110) system and identify stable and metastable adsorption sites. The resulting adsorption energies and equilibrium geometries indicate a tendency to form two-dimensional Sb clusters for submonolayer coverage. The accompanying electronic properties (surface band structure, photothreshold, etc.) are discussed within the context of experimental data available from STM, photoemission spectroscopy, etc.

I. INTRODUCTION

The study of the structural, electronic, and vibrational properties of group-V elements chemisorbed on polar III-V compound semiconductors has attracted much interest in the last decade. Among the most extensively studied interfaces, antimony on cleaved GaAs(110) represents a prototypical system. The chemisorption of column-V semimetals on III-V compounds gives ordered, unreactive, and nondisruptive interfaces for monolayer overlayers, where one monolayer (1 ML) corresponds to 8.85×10^{14} atoms/cm^2 or to an effective coverage $\Theta=1$. The relationship between structural and electronic or vibrational properties can be sketched already in the initial stages of the interface formation. More strictly speaking, Sb/GaAs(110) appears as a model system for studying the relationship of growth, structure, chemical bonding and resulting properties, e.g., the Fermi-level pinning.

Antimony strongly binds to the (110) surface of GaAs. In the submonolayer coverage regime, i.e., $\Theta<1$, antimony adsorbates on GaAs(110) tend to cluster together, forming islands.[1-3] The islands have a height corresponding to 1 ML, i.e., about 2.5–2.8 Å. The island size is of the order of 10–100 Å. Most of these islands represent ordered clusters along the zig-zag chains of cations and anions in the $[\bar{1}10]$ direction. They have a 1×1 unit cell which matches that of the clean GaAs(110). However, around the edge of the Sb islands defects exist. As the islands grow in size these defects persist, generally maintaining their positions at the edge of the Sb terraces. At about 0.7 ML the islands merge together and form a 1×1 continuous network over the surface. The overlayer resulting within this two-dimensional growth is not perfectly ordered. The disorder can be substantially reduced by annealing the film.[4,5] At the completion of 1 ML, Sb atoms build up a structure with high chemical stability and local order, probably periodically arranged so as to resemble the geometry of a GaAs(110) topmost layer.[4,6] Both properties of the structure are due to the formation of strong covalent bonds between the adatoms and the substrate Ga and As atoms along the zig-zag chains. At higher coverages, three-dimensional growth of the semimetal Sb occurs without any exchange reaction with the substrate.[4]

The most widely studied Sb/GaAs(110) interface is the ordered structure with a $p(1\times1)$ symmetry and 1 ML Sb on GaAs(110). Besides scanning-tunneling microscopy (STM) studies[1-3] and older structural analyses by low-energy electron diffraction (LEED),[6] there are also careful recent LEED[7] and x-ray standing wave (XSW)[8] investigations. To explain the experimental data, various structural models have been suggested for the monolayer Sb coverage, i.e., $\Theta=1$. The geometry most widely accepted until 1990 was the *epitaxial continued layer structure* (ECLS). It was proposed heuristically by Swarts, Goddard and McGill[9] assuming that the Sb atoms occupy the "next lattice layer" on a nearly unrelaxed GaAs(110) surface. The resulting Sb chains bridge the GaAs chains of a nearly unrelaxed surface. Therefore, sometimes it is also called *bridging-chain model*.[3] Starting from the LEED data, their own photoemission results, and a fully relaxed surface with completely filled or empty dangling bonds, Skeath and co-workers[10-12] suggested a p^3 *structure* model, where the Sb atoms form chains

similar to that of Ga and As and every second Sb is strongly bound to a Ga substrate atom donating two p electrons into the empty p-type dangling orbital of Ga and one p electron into an Sb-Sb bond orbital. These chains are therefore 180° out of phase in comparison with the corresponding layer of the zinc-blende structure. The Sb s electrons remain in tightly bound lone-pair orbitals. The *epitaxial on top structure* (EOTS)[13] is a special case of the p^3 *structure.* However, the adatoms are assumed to be situated in positions nearly on the top of the unrelaxed surface zig-zag chains of Ga and As atoms. Sb chains in the right phase are considered in the *epitaxial overlapping chain structure* (EOCS).[6] However, they are displaced in the [001] direction to overlap laterally with the underlying substrate chains. Another conceivable model is a *dimer structure*[6] with Sb dimers oriented in the [001] direction above Ga atoms.

The atomic geometry of the semimetal overlayer as well as the underlying substrate are extensively determined for the ECLS model by means of the minimization of the total energy within a tight-binding scheme.[14,15] For this structure results of an *ab initio* pseudopotential calculation[16–18] and of a many-body linear combination of atomic orbitals (LCAO) method[19] exist as well. Recent theoretical work[13] using a slightly modified tight-binding scheme has shown that the total energies of the ECLS and EOTS structures are comparable within the accuracy of the method used. On the other hand, the EOCS is computed to be substantially lower in energy than both the ECLS and EOTS. This energetically favored structure is, however, incompatible with both LEED and STM data. STM micrographs have been satisfactorily interpreted using the ECLS as well as the EOTS.[13] The EOTS seems to give a better fit to the data than the ECLS. Mårtensson and Feenstra[3] have also found that the proposed p^3 model is only marginally incompatible with the experimental data. This is somewhat in contrast to LEED[7] and XSW[8] studies which have strongly supported the ECLS model. We mention that the structural data derived from *ab initio* total-energy calculations also favor the ECLS model over the p^3 structure[17] and the EOTS,[18] respectively.

The comparison of experimental results obtained by STM spectroscopy,[2,3,20] angle-resolved photoemission spectroscopy (ARPES),[21–23] and inverse photoemission (IP)[24] for the electronic structure with band-structure calculations[13–18,25] may be a good indicator for the validity of a bonding model. Core-level spectroscopy[5,12] indicated the existence of at least two chemically distinct Sb species at the interface, while valence-band photoemission spectroscopy[10–12] revealed Sb-induced surface states just below the GaAs valence-band maximum (VBM). Additional information follows from the measurement of band bending by work-function,[26,27] surface-photovoltage,[28] Raman scattering[29,30] and photoemission[31] experiments. Furthermore surface-sensitive high-resolution electron energy loss spectroscopy (HREELS) measurements[32–34] on the system Sb/GaAs(110) grown at room temperature exist. The conclusions about the interface structure are rather limited. However, in recent HREELS[34] a low-energy surface-state transition around 1.55 eV is observed in agreement with reflectance difference measurements.[35] Despite the various studies, there is no clear connection between structural and electronic properties. Empirical tight-binding results[13] for electronic states using both the ECLS and EOTS have been found to be in good agreement with photoemission data. On the other hand, the self-consistent *ab initio* calculations[18] within the ECLS model give rise to band states which better fit to direct and indirect photoemission experiments.[23,24]

In this paper we present accurate self-consistent calculations for the atomic geometry, the adsorption energies, and the electronic structure of the Sb/GaAs(110) system. In Sec. II the theoretical method based on the density-functional theory (DFT) is described. In Sec. III we calculate the equilibrium atomic structure for the five geometry models mentioned above in the monolayer-coverage case, i.e., $\Theta=1$. The models are discriminated according to the adsorption energy, and the resulting band structures are compared with experimental data from STM, ARPES, IP, PES, and HREELS. As an example for the submonolayer adsorption we study the case $\Theta=\frac{1}{2}$ in Sec. IV. In addition to the homogeneous coverage of 1×1 symmetry we also investigate chain and dimer structures of 2×1 or 1×2 symmetry. The preferred adsorption sites of Sb on GaAs(110) and the tendency for clustering are studied. The interface states are discussed in the context of the Fermi-level pinning. Finally a brief summary is given in Sec. V.

II. COMPUTATIONAL METHOD

The parameter-free electronic structure, total energy, and force calculations are performed within the density-functional theory.[36,37] The electron-ion interaction is treated by using norm-conserving, *ab initio,* fully separable pseudopotentials in the Kleinman-Bylander form[38] as given in Ref. 39. They are based on relativistic all-electron calculations for the free atom by solving the Dirac equation self-consistently.[38,40,41] The exchange-correlation functional of the electron-electron interaction is approximated by its local version.[37] Explicitly the electron-gas data of Ceperley and Alder[42] are taken into account in the form as parametrized by Perdew and Zunger.[43]

In order to describe clean and covered semiconductor surfaces we use the repeated-slab method.[44] Each slab contains eight atomic (110) layers of GaAs. Sb atoms are placed on both sides of the slab. We use a vacuum region which has a thickness of six atomic layers. The wave functions are expanded in terms of plane waves. An energy cutoff of 8 Ry is used for the plane-wave basis set, which corresponds to about 1500 plane waves for the 1×1 systems. To make sure that the results are well converged, some of the results are checked by using a cutoff of 18 Ry corresponding to more than 5000 plane waves. The summation over four special $\mathbf{k}$ points[45] in the irreducible part of the surface Brillouin zone was used to replace the Brillouin zone integrations. To improve the $\mathbf{k}$-space sampling we use partial occupation numbers according to a Fermi function with an effective electron

temperature of $k_B T = 0.01$ eV.

The GaAs lattice constant is optimized for a GaAs(110)1×1 slab to a value of 5.5 Å. All results reported hereafter are obtained with this theoretical lattice constant that is somewhat smaller than the experimental value of 5.65 Å. In order to determine the equilibrium atomic positions, the atoms of the three outermost substrate layers and the adatoms on both sides of the slab are allowed to relax to geometries given by the calculated total energies and forces, using a steepest-descent method for the atomic displacements together with a Car-Parrinello-like approach[46] for bringing the wave function to self-consistency. We apply the computer code cp93fhi of Stumpf and Scheffler.[47] The equilibrium geometry is identified when all forces are smaller than 0.05 eV/Å. This corresponds to an uncertainty of the atomic positions of less than 0.01 Å.

In several cases we also derive adsorption energies per Sb atoms. For this purpose we do not only need the total energies of the slab with and without adsorbate. In addition, the energy of free Sb atoms has to be known. It is also calculated by the method described above, but spin-polarization effects are taken into account. Despite the inclusion of spin effects the adsorption energies seem to be overestimated using such a scheme by about several tenth of eV per bond. At the very least, such a value can be derived comparing the theoretical values for the cohesive energy per bond of 2.05 eV (GaAs) or 2.00 eV (GaSb) obtained for fcc structure and 18 Ry cutoff with the corresponding experimental values, 1.63 and 1.48 eV.[48] This overestimation results mainly from the different calculation methods for atomic and solid-state energies. The overestimation of the chemical bonding is indeed another reason as can be seen from the theoretical bond lengths of 2.41 Å (GaAs) and 2.61 Å (GaSb) which are 0.04 Å smaller than the experimental ones.[48] We mention that the overestimation of cohesive energies of semiconductors by roughly 0.5–1.5 eV per atom is well known for the typical DFT-LDA procedures of calculation.[49] Nevertheless, we can use these values since we only consider differences comparing different structures.

III. MONOLAYER COVERAGE ($\Theta = 1$)

A. Adsorption energies and chemical bonds

Proceeding from the five structural models mentioned above for the monolayer Sb coverage and schematically presented in Fig. 1, we find that indeed they give rise to at least local minima in the total-energy surface. Although constraint of symmetry is assumed, these minima indicate the stability of the structures with certain atomic geometries. From the energetical point of view, however, they are of different importance, even when the accuracy of the adsorption energies in Table I is limited. On the other hand, the adsorption energies per additional adsorbate-adsorbate or adsorbate-substrate bond of about 2 eV are of the same magnitude as the cohesion energies found for bulk GaAs and GaSb (cf. Sec. II). Taking into account the typical values for the energy gain due to lattice relaxation from the clean GaAs(110)1×1 surface of 0.7 eV per surface GaAs pair,[50] strong covalent Sb-Sb bonds follow with a similar strength as the Ga-As and Ga-Sb bonds. In the case of the ECLS the covalent bonds can be seen clearly from Fig. 2. We note that for this structure the Sb atoms are linked to the substrate by directional bonds. The total valence-electron density around the atomic connection lines is very similar for Sb-As, Sb-Sb, and Ga-Sb. However, for the Sb-As (Ga-Sb) bond the center of gravity is somewhat shifted from midbond towards the As (Sb) atom, indicating the minor ionic character of these bonds. The direction of these shifts follows the electronegativities 1.81, 2.05, and 2.18 of the atoms Ga, Sb, and As.[51] The electrostatic forces associated with the partially ionic character of the bonds seem to be responsible for the small counter-

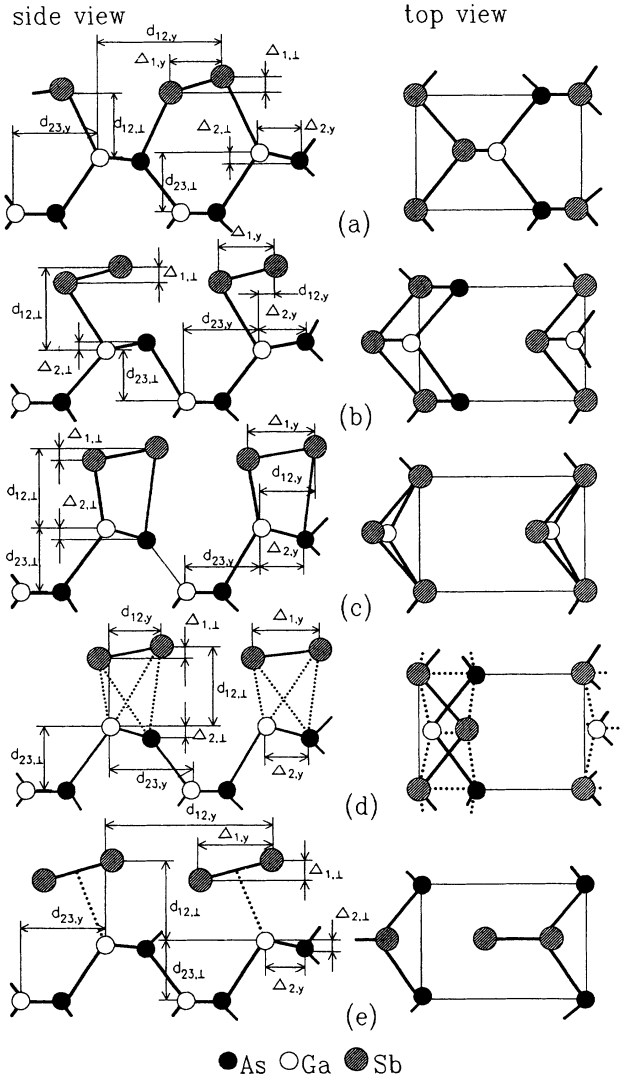

FIG. 1. Schematic representations of side and top views for the five classes of surface geometries for the Sb/GaAs(110)1×1 system with one monolayer antimony: (a) epitaxial continued layer structure (ECLS), (b) p^3 structure, (c) epitaxial on top structure (EOTS), (d) epitaxial overlapping chain structure (EOCS), and (e) dimer model. The notation of atoms is valid throughout the paper.

TABLE I. Adsorption energies per Sb adatom and bond lengths in the first two atomic layers for monolayer Sb/GaAs(110)1×1 systems. The shortest bond length is taken if more than one distance comes into question. The second values for ECLS result from a calculation with the energy cutoff of 18 Ry.

Geometry model	Adsorption energy (eV)	Bond length (Å) Sb-Sb	Ga-Sb	Sb-As	Ga-As
ECLS	$\frac{4.48}{4.42}$	$\frac{2.79}{2.79}$	$\frac{2.55}{2.57}$	$\frac{2.64}{2.64}$	$\frac{2.39}{2.40}$
p^3	4.13	2.83	2.61	2.79	2.39
EOTS	4.23	2.82	2.67	2.77	2.38
EOCS	3.43	3.00	2.81	3.14	2.46
Dimer structure	3.55	2.81	2.76	2.96	2.43

relaxation in the first GaAs layer, although Ga and As are nearly sp^3 hybridized in the ECLS. Together with the covalent radii[51] it also explains the subsequent buckling in the Sb-Sb chains.

The ECLS model, considered theoretically in detail in Refs. 13 and 16–18, is clearly the structure of choice. The EOTS model which perhaps better fits to the STM images[13] as well as the original p^3 structure[3] are only 0.25 and 0.35 eV higher in energy. On the other hand, the EOCS and dimer models seem to fail considering the energetics. It is striking, that the structures, which nearly conserve the bond length close to the sum of covalent radii[51] of 2.80 Å (Sb-Sb), 2.66 Å (Ga-Sb), 2.60 Å (Sb-As), and 2.46 Å (Ga-As), are lower in energy. This holds especially for the three structures, being most favorable from the energetical point of view, although the ordering of the bond lengths Ga-Sb and Sb-As is reversed. In the case of the EOCS and dimer bonding the interface is remarkably expanded, resulting in a lowering of the adsorption energies. A similar argument holds for the energy lowering in the case of the EOTS and p^3 structure. There the Sb-As bond length is much larger than that for the ECLS. It is noteworthy to mention that the Sb-Sb bond length of about 2.8 Å is nearly the same in all structures, apart from the EOCS.

Another interesting insight in the bonding behavior arises from the comparison of the p^3 structure and the EOTS. According to LaFemina, Duke, and Mailhiot,[13] the bonding between the GaAs surface layer and the Sb-Sb chains is also best characterized as a p^3 hybridization, which is responsible for both the intrachain and the overlayer-substrate interactions as already discussed for the p^3 structure. We believe that within the p^3 structure only a strong Ga-Sb substrate-adsorbate bond occurs whereas the bond angles for the Sb p orbital and the near As sp^3 hybrids are unfavorable for a strong bond. In the case of the EOTS Sb atoms can regularly bind to Ga as well as As. Of course, these bonds are somewhat weaker than the Ga-Sb bond within the p^3 structure. Indeed, the Ga-Sb bond length of the p^3 structure is smaller by 0.06 Å than in the EOTS, whereas the Sb-As distance changes by -0.02 Å between these two structures. In our opinion this bonding picture may also explain the missing counter-relaxation for the p^3 structure (cf. Table II). The bonding of the Sb-Sb chain to the As atom is so weak that As tends to occupy a relaxed position similar to that at the clean GaAs(110) surface.

B. Atomic energy

The most important parameters of the atomic geometry of the Sb monolayer and the underlying relaxed GaAs(110) surface are listed in Table II. The structures according to the five different local minima of the total energy are in a qualitatively good agreement with the predictions of Duke *et al.*[6] We find counter-relaxation of the outermost GaAs layer with the only exception of the p^3 structure. The buckling of the Sb chains or dimers is one important structural parameter. This vertical displacement between the two inequivalent Sb atoms per surface unit cell, $\Delta_{1,\perp}$, of 0.05 or 0.06 Å is in good agreement with the LEED analysis[6,7] and other calculations.[13,17,18] The other structural models give, in general, rise to much larger buckling parameters, with the exception of the EOCS. The lateral distance of two Sb atoms in the [001] direction is another parameter of the Sb overlayer. The agreement with LEED results[7] is excellent. However, similar lengths follow also within the EOTS and p^3 structure. An interesting question concerns the buckling $\Delta_{2,\perp}$ in the first GaAs layer. It is reversed (apart from the p^3 structure) but somewhat smaller compared with the clean GaAs(110) surface[52] for reasons discussed

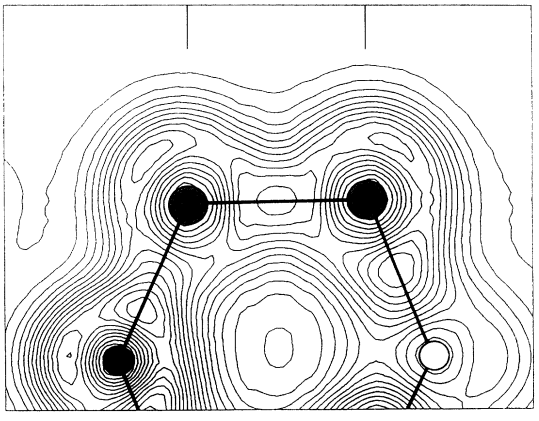

FIG. 2. Contour plots of the valence pseudocharge density for the $\Theta=1$ adsorption of Sb on GaAs(110) in the ECLS. The plots are drawn along the three planes perpendicular to the surface containing the As-Sb, Sb-Sb, and Sb-Ga bonds as indicated by the lines in the upper part of the drawings. The contour step is 0.005 bohr^{-3}.

in Sec. III A. Within the ECLS our value of about 0.1 Å approaches that found by LEED.[7] However, the other structural modes also yield small buckling in agreement with the general tendency of reduction of the GaAs surface relaxation during coverage.[50,53] Such an agreement is also stated for the [001] lateral distance $\Delta_{2,y}$ of Ga and As atoms within the zig-zag chains parallel to the $[\bar{1}10]$ direction. This is more or less valid for all structural models, even if the ECLS should also be favored in this case.

A clear distinction between the structural models arises from the vertical distance $d_{12,\perp}$ of the outwards displaced atoms in the Sb overlayer and the first GaAs plane. Only within the ECLS can the LEED value[7] be reproduced. We mention that the value $d_{12,\perp}=2.35$ Å is also close to the XSW findings[8] of 2.27 ± 0.05 Å for the average vertical distance of Sb atoms from the GaAs surface.

A direct comparison of the data in Table II derived from total-energy minimizations with results of STM is rather toilsome. The experimentalists are not able to observe the lateral position in the $[\bar{1}10]$ direction for the Sb atom closer to the As atom or even bonded to the As atom. Thus, there is an uncertainty which extends over the entire surface unit cell. Nevertheless, one is in a position to compare STM data[3] with results for the lateral distances from total-energy calculations or other methods, e.g., LEED.[7,13] Such a comparison is shown in Fig. 3. We see that the epitaxial overlapping chain structure (EOCS) and the dimer model completely fail such a comparison. Both the ECLS and the EOTS cannot be excluded by such a comparison, although the EOTS seems to be somewhat more reasonable. However, the p^3 structure can also be a structural candidate, even if the agreement is poorer. These conclusions are in agreement with the findings of Mårtensson and Feenstra[3] as well as LaFemina, Duke, and Mailhiot.[13] Nevertheless, we have to mention that, although STM measurements suggest

TABLE II. Structural parameters (cf. Fig. 1) in Å for the five geometries of the system Sb/GaAs(110)1×1 in the monolayer case. The present results obtained for $\frac{8}{18}$ Ry cutoff energy are compared with results of the LEED analysis by Ford *et al.* (Ref. 7), the tight-binding calculations of LaFemina, Duke, and Mailhiot (Ref. 13), the *ab initio* pseudopotential calculations by Srivastava (Ref. 17), and the XSW studies of Kendelewicz *et al.* (Ref. 8).

	ECLS	p^3 structure	EOTS	EOCS	Dimer model
Present results $\Delta_{1,\perp}$	$\frac{0.05}{0.06}$	0.70	0.15	0.08	1.25
LEED[7]	0.08				
Tight binding[13]	0.04		0.33	0.13	
ab initio[17]	0.04	0.66			
Present results $\Delta_{1,y}$	$\frac{2.00}{2.00}$	1.94	2.04	2.28	2.52
LEED[7]	1.99				
Tight binding[13]	1.86		1.83	2.11	
ab initio[17]	1.91	1.93			
Present results $d_{12,\perp}$	$\frac{2.35}{2.36}$	2.89	2.73	2.43	2.76
LEED[7]	2.34				
Tight binding[13]	2.35		2.93	2.11	
ab initio[17]	2.36				
XSW[8]	2.27				
Present results $d_{12,y}$	$\frac{4.51}{4.50}$	0.52	1.41	1.41	5.56
Tight binding[13]	4.47		1.25	1.74	
Present results $\Delta_{2,\perp}$	$\frac{0.08}{0.10}$	0.23	0.03	0.04	0.06
LEED[7]	0.11				
Tight binding[13]	0.03		0.27	0.16	
ab initio[17]	0.09				
Present results $\Delta_{2,y}$	$\frac{1.38}{1.40}$	1.37	1.36	1.50	2.74
LEED[7]	1.40				
Tight binding[13]	1.41		1.32	1.69	
ab initio[17]	1.43				
Present results $d_{23,\perp}$	$\frac{1.96}{2.00}$	1.73	1.95	1.96	2.00
Present results $d_{23,y}$	$\frac{2.71}{2.70}$	2.76	2.71	2.80	2.76

the atomic positions as in Fig. 3, carefully speaking, these experiments probe the local density of electronic states and not necessarily the positions of cores.

C. Surface band dispersion and orbital character

In Fig. 4 we show the surface band structures computed for the five different overlayer models given in Fig. 1 and described in more detail in Table II. More strictly speaking, we show the dispersion of the surface bound states along high-symmetry lines in the surface Brillouin zone together with the bulk band structure projected onto the (110) plane.

Because of the different bonding behavior in the different models there are only a few similarities in the band structures shown in Figs. 4(a)–4(e). The first three model structures give rise to semiconducting interfaces. Occupied and empty surface bands appearing within the fundamental gap of the projected band structure are well separated energetically. On the other hand, the band structures in Figs. 4(d) and 4(e) indicate a metallic character of the interfaces if EOCS or dimer geometries occur. The s-type interface states S_1 and S_2 appear for all structures (apart from the EOCS) in the ionic gap of the projected band structure. On the other hand, the higher-lying energy bands S_3 to S_8 exhibit a stronger p-type character. This holds especially for the Sb contributions to the corresponding orbitals independent of the overlayer model, whereas the substrate contribution to the interface bonds is nearly represented by sp^3 dangling hybrids, at least for models with an almost unrelaxed first GaAs plane. The pronounced changes for the Sb contributions more concern the hybridization degree. For instance, the ECLS is characterized by p^2 bonding within the Sb chains and Sb p_π contributions to the interface bonds. In the EOTS, however, the intrachain and overlayer-substrate bondings are characterized by a p^3 hybridization of Sb atoms.

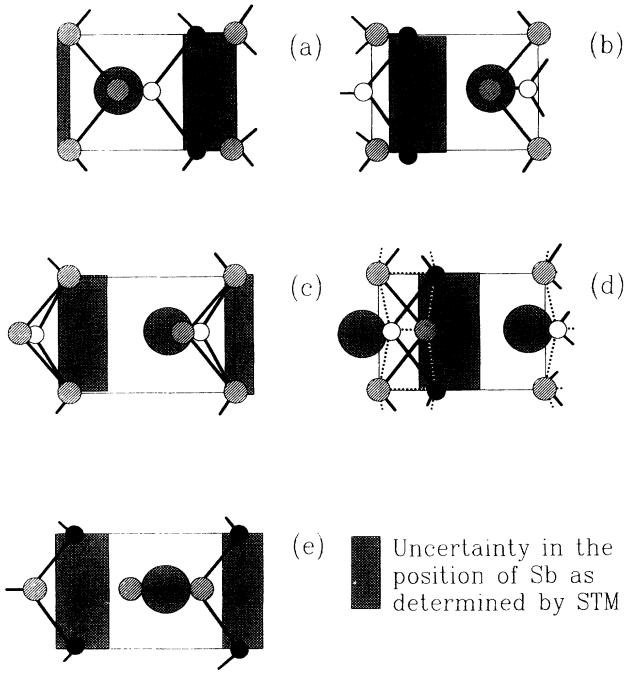

FIG. 3. Comparison of the spatial locations of the topographic features observed in the STM images by Mårtensson and Fenstra[3] with the fully relaxed positions derived by total-energy minimization for different structural models: (a) ECLS, (b) p^3 structure, (c) EOTS, (d) EOCS, and (e) dimer model.

As an example, the orbital character of the two-dimensional Bloch states at (or near) the $\bar{M}$ point of the surface Brillouin zone is plotted in Fig. 5 for the ECLS. Indeed the S_1 and S_2 states are almost localized at one of the two differently bonded overlayer atoms. The orbitals are essentially s like, even if there is also a small back-bond character. The states S_3 and S_4 appear in the pocket of the projected band structure. They belong to bonding combinations of Sb states with As or Ga sp^3 dangling hybrids. However, there are also remarkable contributions to As or Ga states within the corresponding vertical zig-zag chains parallel to [110]. The states S_5 and S_6 exhibit a strong p character, where the p orbitals are nearly parallel to the surface normal. These p orbitals are not only localized at a Sb atom. Rather, there are also contributions from substrate As and Ga atoms. The interpretation of the S_7 and S_8 states is somewhat more complicated. They seem to be characterized almost by antibonding combinations of Sb-As and Sb-Ga states. The principal interpretation of these surface states is similar than that previously given on the base of tight-binding or DFT-LDA calculations.[13,15,25] The discrepancies probably arise from the slightly different geometries used in the electronic-structure calculations.

The most important features in the electronic structures are the Sb-related surface energy bands S_5 to S_8 within the fundamental gap. The energy location and dispersion of the bands vary with the overlayer structure (cf. Fig. 4). Here we focus our attention to the ECLS and EOTS, i.e., the most favorable structures from the energetical and structural point of view. Unfortunately, experimental results for the unoccupied surface states are available only for few $\mathbf{k}$ points.[24] Therefore, it is not clear if the S_7 band exhibits a minimum near $\bar{X}$ and if the strong dispersion along the $\bar{\Gamma}\bar{X}$ line is an artifact of the calculation. In any case, the ECLS gives rise to a pronounced dispersion of S_7 and S_8 along $\bar{\Gamma}\bar{X}$ whereas this dispersion is remarkably reduced in the EOTS case. A more detailed comparison with experimental results[22,23] is possible in the case of the highest occupied surface states S_3, S_4, A_2, S_5, and S_6, as shown in Fig. 6. We find that the photoemission results agree better with the band-structure calculation for the ECLS geometry. The dispersion of the nearly degenerated S_3 and S_4 bands is perfectly reproduced. In the case of S_5 and S_6 the principal behavior is comparable, especially when the anion-related band A_2 is taken into discussion. However, it is worth mentioning that the theory underestimates the dispersion found experimentally. In particular, the splitting between the S_5 and S_6 bands near $\bar{X}$ and $\bar{X}'$ seems to be underestimated. On the other hand, our results seem to fit better the experiment than previous band-structure

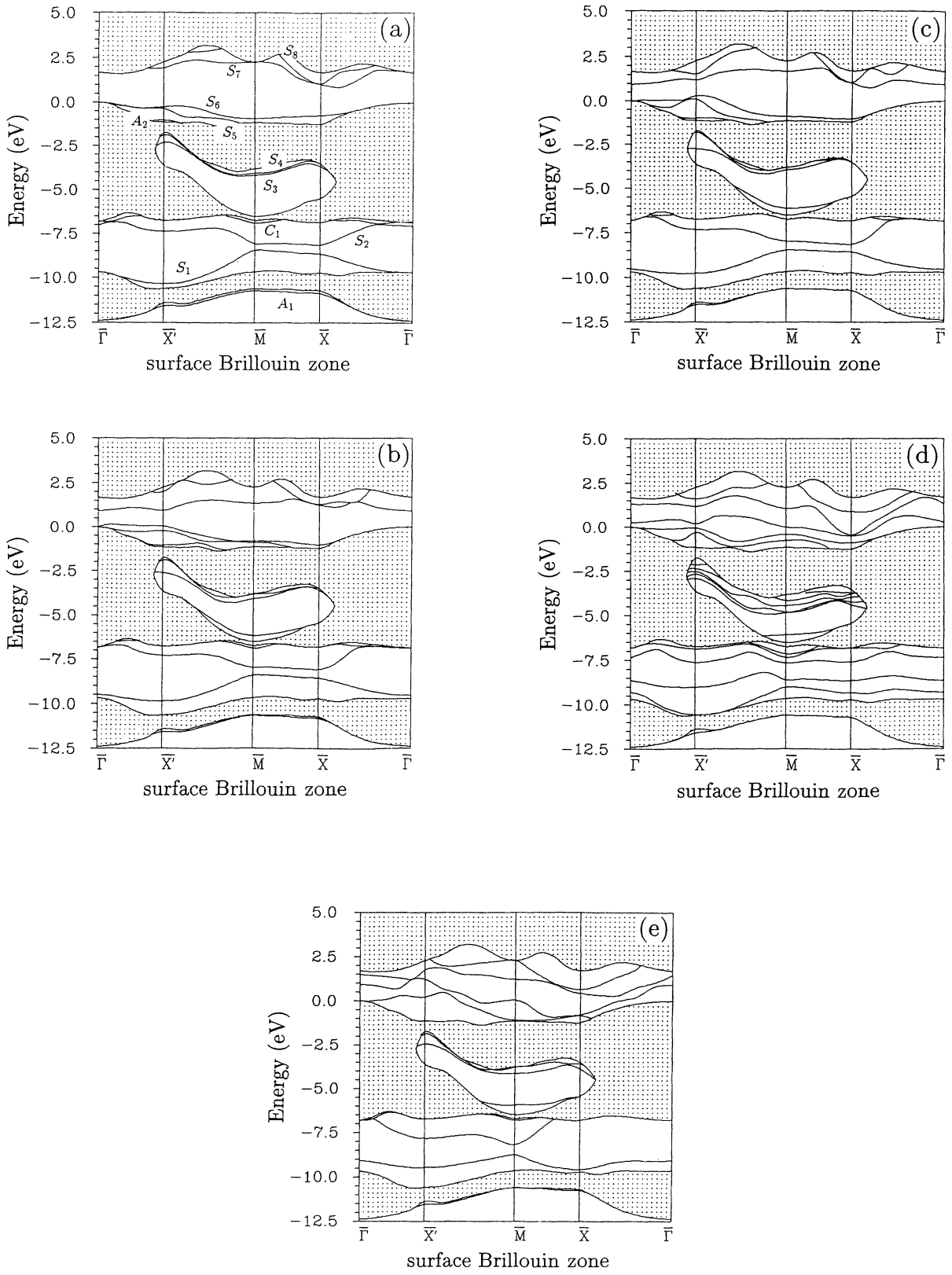

FIG. 4. Surface band structure (bound states) for Sb/GaAs(110)1×1 (1 ML) plotted over the projected bulk band structure of GaAs (dotted region). Five different structures are considered. (a) ECLS, (b) p^3 structure, (c) EOTS, (d) EOCS, and (e) dimer model. Sb-related surface bands are labeled by S_n, whereas substrate anion-(As) and cation-(Ga) derived surface states are denoted by A_n and C_n, respectively. The index n counts the bands according to their energetical position. All energies are referred to the valence-band maximum.

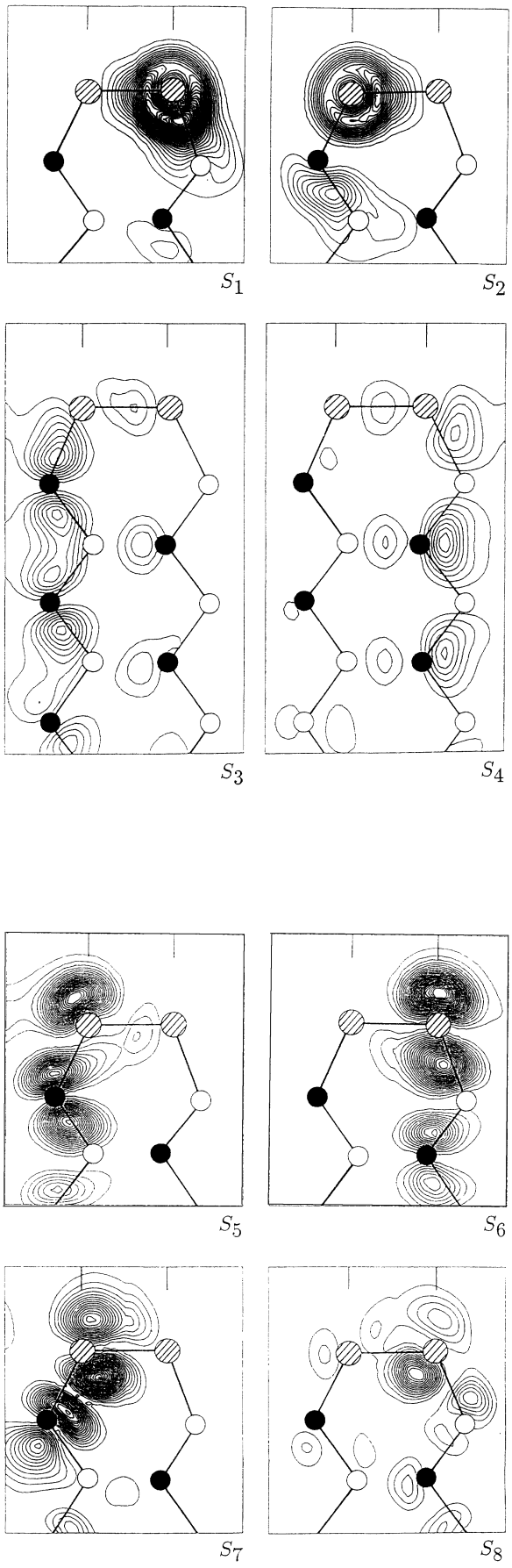

calculations.[13,15,25] This holds especially for the S_3/S_4 bands, the dispersion of which is excellently reproduced. We trace this fact back to the use of a geometry optimized by *ab initio* total-energy calculations. The most important fact, contradicting the validity of the EOTS, is the strong dispersion of $S_{5,6}$ near $\bar{X}'$. The appearance of the valence-band maximum (VBM) at $\bar{X}'$ is not in agreement with experimental findings.

D. Energy levels and excitation energies

For Sb monolayers on GaAs(110) a variety of experimental studies including STM spectroscopy,[20] spectroscopic ellipsometry,[27] HREELS,[34] reflectance difference spectroscopy,[35] as well as resonance Raman scattering[30] have reported electronic transitions between surface bands. Table III presents a collection of these results. The experimental results are energetically ordered and arranged in groups of similar values. The transition energies of about 2.25, 2.65, 3.2, and 3.75 eV are reproducibly observed within the different excitation spectroscopies. They should therefore be attributed to maxima in the combined density of states of the monolayer Sb/GaAs (110) system. Considering the band structures in Fig. 4 the listed energies can be assigned to transitions between the filled (S_5 and S_6) and empty (S_7 and S_8) surface bands, that essentially originate from the Sb-As (S_5,S_7) and Ga-Sb (S_6,S_8) backbonds or antibackbonds. A detailed identification between the transitions and the specific surface bands is, however, difficult since the symmetry of the initial and final states involved in the experiment is unknown or only average positions follow from the experiment (cf. STM). Looking at the theoretical band structures in Fig. 4 only direct transitions at critical points on the boundary of the surface Brillouin zone should occur. Within the ECLS the bands S_6 and S_7 really describe surface bands at these **k** points. S_5 (S_8) gives rise to pronounced bound states only near $\bar{X}'$ ($\bar{X}$). Considering this fact and the orbital character of the states we give in Table III only calculated energies for the transitions $S_5 \rightarrow S_7$ at $\bar{X}'$, $\bar{X}$, and $\bar{M}$ as well as $S_6 \rightarrow S_8$ at $\bar{X}$ and between $\bar{X}'$ and $\bar{M}$. The theoretical values cover the most important experimental transition range between 1.9 and 3.75 eV. The onset of transitions found in HREELS of 1.55 eV is rather small. It can only be related to weak $S_6 \rightarrow S_7$ transitions on the $\bar{X}\bar{\Gamma}$ line. However, the experimental finding should better be related to surface-state-bulk-band transitions. The inclusion of strong excitonic effects shifting optical transition energies by the electron-hole-pair binding energy to smaller values could be another possibility for lifting the conflicting con-

FIG. 5. Contour plots of the squared wave functions for the ECLS of Sb/GaAS(110)1×1 at (or near) the $\bar{M}$ point in the surface Brillouin zone for the bound surface states S_1 to S_8. Contours are spaced in units of 10^{-3} bohr^{-3}. The plots are drawn along the 3 planes containing the As-Sb, Sb-Sb, and Sb-Ga bonds as indicated by the vertical lines in the upper part of each panel. Large patterned circles indicate Sb atoms, As are marked by dots, and Ga atoms are represented by small circles.

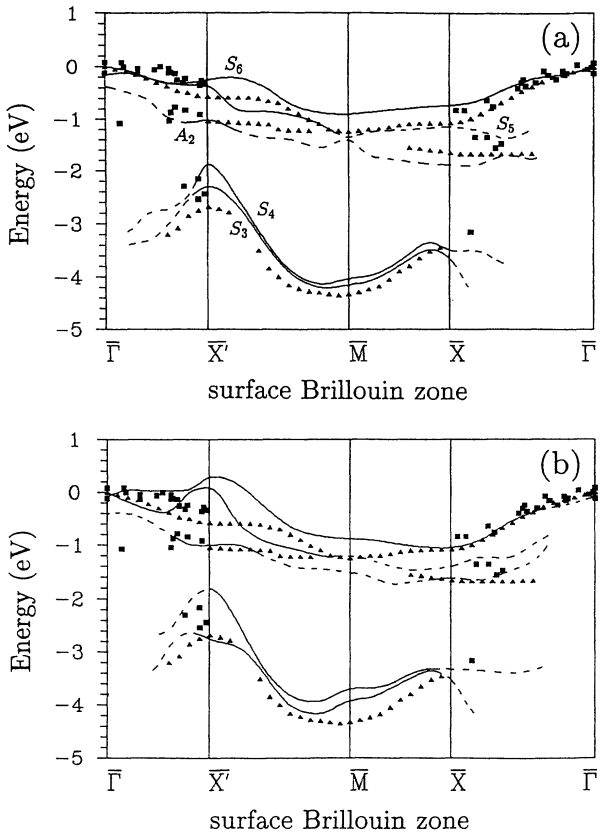

FIG. 6. Comparison of the dispersion of surface bands for Sb/GaAs(110)1×1 ($\Theta=1$) computed for (a) ECLS and (b) EOTS models with ARPES values of Refs. 21, 22 (squares), and 23 (triangles). Solid lines indicate bound states whereas dashed lines denote resonance states. The theoretical and experimental values are aligned at the highest occupied surface state at 0 eV at $\bar{\Gamma}$.

clusions. The comparison between theory and experiment is also complicated because of the quasiparticle problem involved in the excitation spectroscopies.[54,55] However, in our DFT-LDA slab calculation this problem is of minor importance since we start already with a nearly correct gap for bulk GaAs.

Despite the absence of the bulk-gap problem, an indication of quasiparticle effects results from the consideration of the lowest empty surface states. Inverse photoemission[23] observes these states at 2.1 eV above VBM at $\bar{\Gamma}$ within the projected bulk bands. In our DFT-LDA calculation we find this energy level only 1.8 eV above VBM. The calculated S_7 band along the $\bar{\Gamma}\bar{X}$ line seems to be too low in energy. Especially, the appearance of S_7 and S_8 near $\bar{X}$ in the fundamental energy gap in all DFT calculations[17,18,25] should be interpreted as an artifact of the calculations. Such levels are not observed within the measurements of the Fermi-level pinning.[26–28]

Another interesting energy level is the valence-band maximum (VBM). Relative to the vacuum level (given by the effective potential outside the slab) it gives the ionization energy of the system under consideration. This quantity was found to be sensitive with respect to the thickness of the vacuum. In order to avoid interactions through the vacuum region, the length of the supercell was taken to be 90 bohr. The reduction of the ionization energy during monolayer Sb coverage can be simply derived studying the highest occupied band state. Relative to the clean GaAs(110)1×1 surface we derive changes of −0.56 (ECLS), −1.11 (p^3 structure), −0.72 (EOTS), −1.32 eV (EOCS), and −1.19 eV (dimer). These values are indeed smaller than the difference of the GaAs(110)1×1 ionization energy of 5.47 eV and the Sb-semimetal work function of 4.05 eV. The reduction of the ionization energy is due to the changed surface dipole. In Fig. 7 we have shown the difference of the electrostatic potentials of the clean GaAs(110)1×1 surface and the 1 ML Sb/GaAs(110)1×1 system (ECLS). The variation of the potential difference from the vacuum region through the interface into the bulk corresponds to a surface dipole of about 0.4 eV. The difference of this value to the reduction of the ionization energy calculated via the VBM indicates the limited accuracy of the slab calculations. However, we think that even from the consideration of the changes of the ionization energies the ECLS should be favored. The theoretical value for the change of the ionization energy ΔI of about −0.5 eV is closer to the experimental value of −0.3 eV (Ref. 26) than the numbers evaluated for the other structures.

TABLE III. Transition energies (in eV) derived from various experimental techniques as STM spectroscopy (Ref. 20), spectroscopic ellipsometry (Ref. 27), reflectance difference spectroscopy (Ref. 35), HREELS (Ref. 34), and resonance Raman scattering (Ref. 30). They are compared with results of band-structure calculations (ECLS model) for several direct transitions between near surface bound states localized at the same atoms.

Method	Transition energy					
STM			2.2	2.7	3.1	3.7
Ellipsometry				2.65	3.2	3.75
Reflectance			2.25	2.65		
HREELS	1.55	1.9	2.3	2.6	3.2	3.6
Raman			2.2–2.4			
Band structure		$S_6\rightarrow S_8$ ($\bar{X}$)	$S_5\rightarrow S_7$ ($\bar{X}$)		$S_6\rightarrow S_8$ ($\bar{X}'\bar{M}$)	$S_5\rightarrow S_7$ ($\bar{M}$)
(ECLS)		1.82	2.20			3.69
			$S_5\rightarrow S_7$ ($\bar{X}'$)		3.1–3.8	
			2.32			

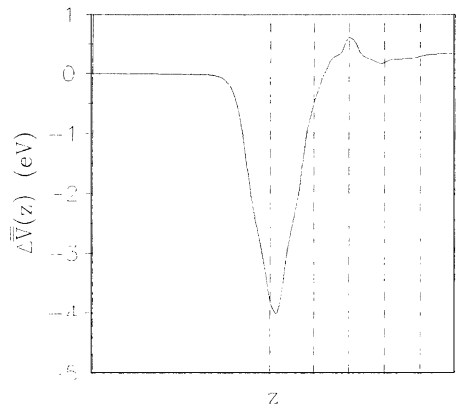

FIG. 7. Difference of the averaged electrostatic potential $\Delta\bar{\bar{V}}(z)$ for 1 ML Sb/GaAs(110) (ECLS) and the clean relaxed GaAs(110)1×1 surface versus the coordinate perpendicular to the surface. Dashed lines mark the averaged positions of the Sb and GaAs layers, respectively.

IV. SUBMONOLAYER COVERAGE ($\Theta=\frac{1}{2}$)

A. Born-Oppenheimer energy surface and diffusion

In this section we study a class of structures that are defined by half-monolayer coverage of atomic Sb on GaAs(110). The examination of such structures is motivated by different reasons. One concerns the inevitable uncertainties in specifying the absolute surface coverage. Among other things this holds, for example, for the coverage within the islands appearing in the first stages of the interface formation. A second point arises from the possibility that one adsorbed Sb species observed in experiment was ordered but the second one was disordered at room temperature. The physical reasons for the observed tendencies for clustering and disorder are unknown. A third question concerns the preferred equilibrium adsorption positions in the low-coverage regime.

In order to answer these questions we evaluate the adsorption energy (or total energy of the system) for more than thirty adatom positions within the irreducible part of the two-dimensional 1×1 surface unit cell for $\Theta=\frac{1}{2}$, i.e., one Sb atom per GaAs surface pair. Thereby the adsorbate coordinates are fixed parallel to the GaAs(110) surface whereas both the adsorbate-surface distance and the atomic positions of the top three substrate layers are fully relaxed. The resulting Born-Oppenheimer energy surface of a surface Sb atom is shown in Fig. 8. For a clearer presentation the energy is plotted versus an area of two surface unit cells, together with the surface Ga-As atomic chains, in the lower panel of the figure. A contour plot of this energy surface is given in the upper panel of Fig. 8. The most pronounced feature of the total-energy surface is the deep channel which is quite rectilinear and parallel to the $[\bar{1}10]$ direction, i.e., the direction of the GaAs zig-zag chains. The absence of minima localized in front of the Ga and As dangling bonds, respectively, is somewhat unexpected. In the case of sodium on GaAs(110) such minima have actually been found.[56] We relate these findings to the simpler electronic structure of the alkali atoms. Because of the five valence electrons Sb tends to adsorption sites with higher coordination. Indeed we find two equivalent energy minima in between an As atom and the two opposite Ga atoms from the neighbored zig-zag chain. These long-bridge-bond positions of an Sb atom between Ga and As atoms of different surface chains are also somewhat in contrast to the self-consistent LCAO studies of the same overlayer structure,[19] which found a somewhat displaced adsorption site giving rise to a threefold coordination of Sb between two Ga atoms of one chain and the corresponding As atom of the neighbored chain.

The bonding properties of the Sb adatom in one of the two equilibrium positions are shown in Fig. 9 in more detail. From the side view of the valence electron density [Fig. 9(a)] the long bridge bond consisting of a Ga-Sb and a Sb-As bond with bond lengths of 2.88 and 2.74 Å is observable clearly. They form an angle of about 101° at the Sb adatom indicating that a mixture of Sb p_σ and sp^3 bonds are involved. The lower panels [Figs. 8(b)–8(d)] indicate two facts. First, the adatom position is not situated on a straight line between Ga and As. The adatom is slightly displaced in the $[\bar{1}10]$ direction towards the [001] connection line of two As atoms. Second, there is a cer-

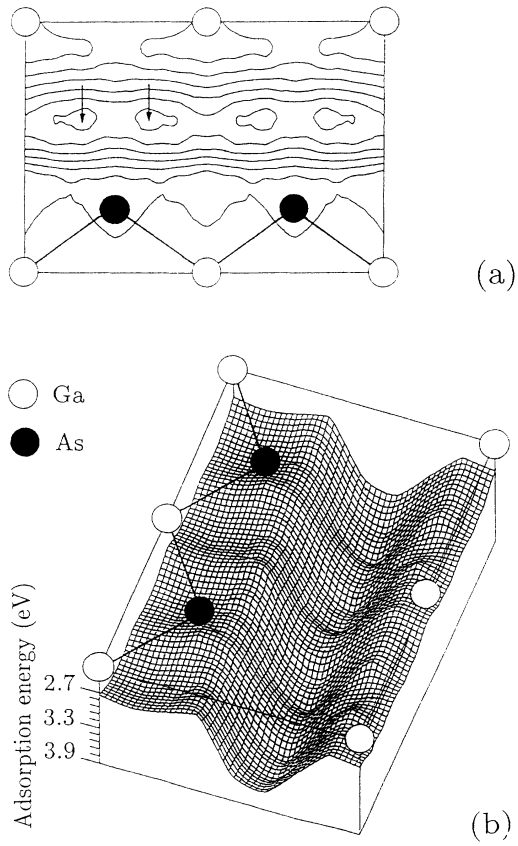

FIG. 8. Total-energy surface of the ($\Theta=\frac{1}{2}$) Sb/GaAs(110) system is plotted over an area of two GaAs surface unit cells as a contour plot (a) and as a three-dimensional perspective view (b). The two flat equivalent minima per unit cell between As and Ga atoms are marked by arrows in the upper panel.

tain overlap of Sb p_π orbitals localized in different unit cells. The Sb atoms are in the [$\bar{1}$10] direction in a distance of 3.9 Å. This overlap might explain the relatively large adsorption energy of about 2.7 eV even on the plateaulike barrier regions of the energy surface on top of the Ga-As zig-zag chains.

The particular form of the energy surface allows important conclusions concerning a highly anisotropic diffusion of the Sb atoms at the GaAs(110) surface. The variation of the total energy along the channel is small. The equivalent minima are separated by barriers of 0.18 eV between two As atoms in the [001] direction and 0.35 eV between two Ga atoms in this direction. Perpendicular to the channel, i.e., in the [001] direction, the energy barrier is calculated to be about 1.2 eV. Since the energy barriers $E_{\parallel,\perp}$ strongly modify the temperature dependence of the diffusion coefficient $D_{\parallel,\perp} \sim \exp(-E_{\parallel,\perp}/k_B T)$ one expects widely different diffusion lengths $l_{\parallel,\perp} = (D_{\parallel,\perp}\tau)^{1/2}$ parallel and perpendicular to the channel within a certain diffusion time interval τ. For room temperature the ratio of the two lengths should therefore be nearly $l_\parallel / l_\perp \approx 10^7$. We mention that the STM images[2] in the low-coverage regime seem to indicate islands the extent of which in the [$\bar{1}$10] direction is larger than in the [001] direction.

Another conclusion follows from the two equivalent adsorption sites for the single Sb atom per unit cell. This fact can be related to a tendency for disorder effects during the submonolayer coverage, more strictly speaking, for a nonhomogeneous distribution of the Sb atoms over the GaAs(110) surface. The existence of two energetically equivalent minima may cause a symmetry break leading to a lowering of surface translational symmetry, i.e., reconstruction or even a destroying of the translational symmetry, i.e., clustering. This conclusion is also supported by the relatively small adsorption energy of 3.89 eV in comparison to the corresponding value of 4.48 eV for the $\Theta = 1$ coverage (ECLS model) which makes other structures more favorable from the energetical point of view.

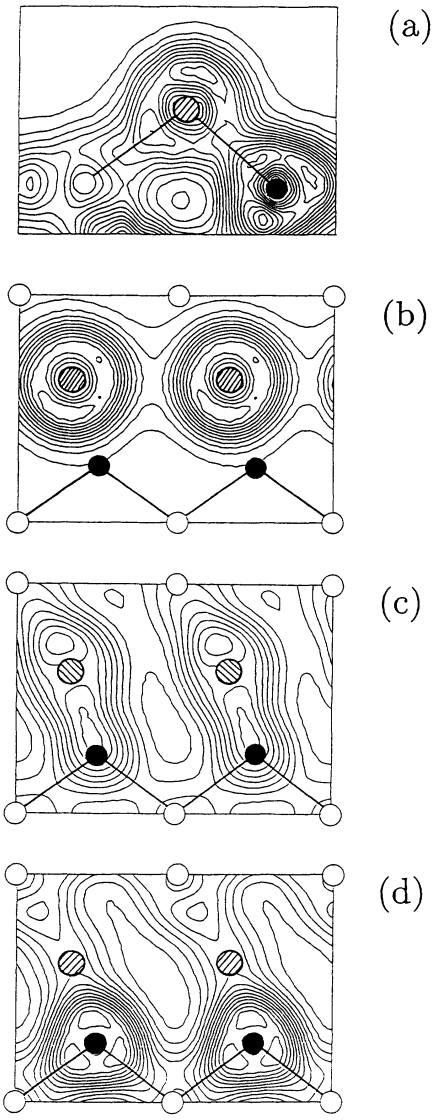

FIG. 9. Contour plot of the total valence-pseudocharge density for the system Sb/GaAs(110)1×1 with ($\Theta = \frac{1}{2}$). In (a) the upper panel, the density is plotted along a plane vertical to the surface containing the bonds from the adatom to both the As and Ga atoms. In the lower panels the density is drawn along (b) (110) planes 0.6 Å above, (c) 0.5 Å below, and (d) 1.1 Å below the Sb adatom cores. The contours are spaced by 0.005 bohr^{-3}.

B. Overlayer reconstruction

Based upon the results presented in Fig. 8 we have additionally studied three 2×1 or 1×2 reconstructed Sb/GaAs(110) surfaces for the half-monolayer coverage in more detail. They are shown in Fig. 10. The three

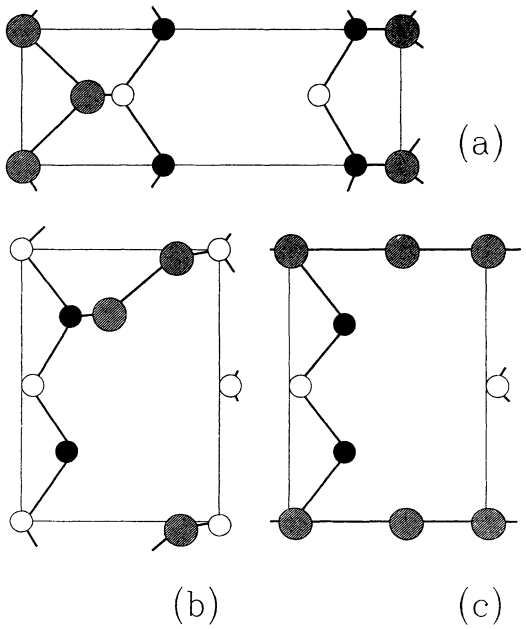

FIG. 10. Considered reconstructed geometries for the Sb/GaAs(110) with $\Theta = \frac{1}{2}$ (top view) with (a) 2×1 or (b) and (c) 1×2 symmetry.

structures considered consist of Sb chains of different form, orientation and Sb-Sb bond length. Figure 10(a) represents an ECLS model where every second Sb-Sb zig-zag chain parallel to the $[\bar{1}10]$ direction is missing. Zig-zag chains parallel to the [001] direction with Sb adatoms bonded to the Ga and As dangling bonds are drawn in Fig. 10(b). Linear chains of Sb atoms grown in [001] direction on top of each second row of Ga atoms are assumed in the geometry of Fig. 10(c). All structures give rise to local minima in the total energy. The adsorption energies per Sb atom resulting for the three structures are 4.25, 3.83, or 3.46 eV. That means the 2×1 zig-zag chain structure turns out to be remarkably more favored from the energetical point of view over the two 1×2 structures under consideration. However, this also holds with respect to the 1×1 structure studied for the same coverage $\Theta=\frac{1}{2}$. The energy gain compared with this structure is about 0.4 eV.

In conclusion, comparing the 2×1 structure and the 1×1 geometry we find the energetical favoring of an inhomogeneous coverage versus the homogeneous distribution of the adatoms in the submonolayer case, at least for $\Theta=\frac{1}{2}$. This can again be interpreted as a physical reason for a tendency towards the formation of flat clusters. In order to discuss the structure of such clusters we first compare the adsorption energies for the $\Theta=1$ and $\frac{1}{2}$ cases. Taking into account only the most favorable structures, i.e., the ECLS model in the monolayer case and the 2×1 missing-chain structure for $\Theta=\frac{1}{2}$, we find that the adsorption energy in the first case is with 4.48 eV slightly larger than the 4.25 eV calculated for the 2×1 geometry. This result can be interpreted in terms of practically noninteracting Sb-Sb zig-zag chains parallel to the $[\bar{1}10]$ direction. Their distance in the [001] direction amounts to nearly 5.5 Å within the ECLS. The slight energy difference arises from slightly differently relaxed surface geometries as well. If changes in the energetics of the clusters due to boundary effects can be neglected, the theoretical results should be interpreted that in the effective submonolayer case the formation of flat islands with local 1×1 symmetry and local $\Theta=1$ coverage is favored. This conclusion is apparently in agreement with the experimental findings.[1-3] A clear discrimination of the 2×1 missing-chain structure is seemingly possible. The energy difference of 0.23 eV per atom is somewhat larger than the uncertainty of the theory.

C. Geometry of the missing-chain structure

Since the appearance of the missing-chain structure with 2×1 symmetry cannot be completely excluded in the submonolayer regime, especially not for nominal $\Theta=\frac{1}{2}$ coverage, we present and discuss the resulting relaxed geometry. A more detailed schematic description of this structure is given in Fig. 11(a). For completeness, the 1×1 long-bridge-bond structure for the same average coverage $\Theta=\frac{1}{2}$ is also given [Fig. 11(b)]. The corresponding geometry parameters as derived from the total-energy optimizations are listed in Table IV.

We observe characteristic discrepancies between the two $\Theta=\frac{1}{2}$ structures under consideration. For the 1×1 geometry the relaxation of the first GaAs(110) layer is lifted. The structure is characterized by a small counter-relaxation of 0.07 Å and a lateral displacement of the As atom towards the Sb of about 0.22 Å. In the 2×1 case some features known from the free surface are reproduced in the outermost substrate layer. It is relaxed with buckling parameters $\Delta_{2,\perp}^{(1)}=0.42$ Å and $\Delta_{2,\perp}^{(2)}=0.18$ Å which are somewhat reduced with respect to the corresponding parameter[52] for the GaAs(110)1×1 surface. As a consequence the reversed buckling is also observed for Sb-Sb zig-zag chains in the 2×1 geometry, at least with respect to the ECLS of the full monolayer coverage. In contrast to the ECLS, now the Sb atom bonded to As is displaced outwards, whereas the other Sb atom bonded to Ga is shifted towards the substrate. Nevertheless, the bond lengths are again nearly conserved. In the first two atomic layers of the 2×1 structure we find the values

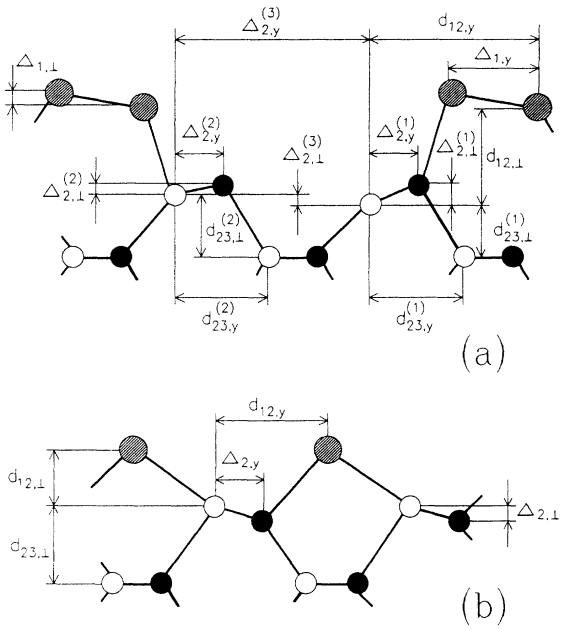

FIG. 11. Side view of (a) the 2×1 missing-chain structure and (b) the 1×1 long-bridge-bond structure for the Sb/GaSb(110) ($\Theta=\frac{1}{2}$) system.

TABLE IV. Structural parameters (cf. Fig. 10) in Å for the 1×1 long-bridge-bond structure and the 2×1 missing-chain structure of the Sb/GaAs(110) ($\Theta=\frac{1}{2}$) system. Note that the sign convention for $\Delta_{1,\perp}$ is opposite to Fig. 1 and Table I.

	1×1 structure		2×1 structure	
$\Delta_{1,\perp}$			0.14	
$\Delta_{1,y}$			1.97	
$d_{12,\perp}$	1.74		2.68	
$d_{12,y}$	3.50		4.38	
$\Delta_{2,\perp}^{(i)}$	0.07	0.42	0.18	0.32
$\Delta_{2,y}^{(i)}$	1.56	1.22	1.32	5.49
$d_{23,\perp}^{(i)}$	2.07	1.61	1.80	
$d_{23,y}^{(i)}$	2.62	2.64	2.50	

$d_{Sb\text{-}Sb}=2.78$ Å, $d_{Ga\text{-}Sb}=2.61$ Å, $d_{Sb\text{-}As}=2.73$ Å, and $d_{Ga\text{-}As}=2.34$ or 2.36 Å. The corresponding values in the 1×1 case ($\Theta=\frac{1}{2}$) are $d_{Ga\text{-}Sb}=2.88$ Å, $d_{Sb\text{-}As}=2.74$ Å, and $d_{Ga\text{-}As}=2.39$ Å. An Sb-Sb bond does not occur. It is, in particular, evident that the Sb-Sb zig-zag chain parameters in the 1×1 ECLS ($\Theta=1$) and the 2×1 missing-chain structure ($\Theta=\frac{1}{2}$) are actually the same. The Sb-Sb bond lengths (cf. Table I) nearly agree. Only the vertical distance of the Sb-Sb chains to the substrate are slightly increased for the more open $\Theta=\frac{1}{2}$ system.

V. SUMMARY

We have applied the density-functional theory in its local version to calculate the atomic geometry and the electronic structure for antimony-covered GaAs(110) surface by total-energy minimizations using a Car-Parrinello-like technique.[47] It turns out that the atomic geometry of the surfaces depends on the degree of the group-V semimetal coverage.

For submonolayer coverages, for which the interaction of the Sb atoms may be neglected, the relaxation of the clean surface is lifted at the adsorbate nearest neighbors. In this case Sb atoms should form long-bridge bonds with Ga and As atoms of parallel zig-zag chains. The topology of the total-energy surface in this case indicates that the antimony atoms can move rather freely on the GaAs(110) surface. However, the diffusion should be extremely anisotropic. More strictly speaking, an antimony atom migrates along the $[\bar{1}10]$ direction. In agreement with STM observations[1-3] we find several energetical reasons that a more or less inhomogeneous distribution of the Sb atoms over the GaAs(110) is favorable. The two equivalent adsorption positions derived for $\Theta=\frac{1}{2}$ and 1×1 symmetry indicate a possibility for lowering the total energy by reducing the translational symmetry. Another indication for favoring the formation of flat clusters with monolayer thickness is the fact that a 2×1 missing-chain structure gives rise to a higher adsorption energy than a homogeneous Sb distribution. We recommend more detailed experimental studies of the cluster structure and the cluster growth in the submonolayer regime.

After extensive studies of five structural models for $\Theta=1$ we favor a structure of the full antimony monolayer prefixed by a layer-by-layer growth, i.e., the epitaxial continued layer structure (ECLS). However, from energetical reasons the epitaxial on-top structure (EOTS) cannot be completely excluded. Nevertheless, we find that the geometry optimized within the ECLS model by the total-energy minimization gives a good agreement with results of the LEED analysis. Moreover, the resulting occupied surface bands reproduce the dispersion found within ARPES in a reasonable manner. Of course, the agreement is not complete. Differences occur with respect to the strength of the dispersion of the $S_{5,6}$ bands. The same holds for the optical excitation energies. Some but not all features can be reproduced. Even in this case more detailed studies of the frequency behavior and the polarization dependence of the optical constants[57] are necessary.

ACKNOWLEDGMENTS

It is a pleasure to thank J. Hebenstreit, M. Scheffler, G. P. Srivastava, and R. Stumpf for many valuable discussions and their help with the computer code. We thank P. Käckell for the assistance in the calculation of adsorption energies. We would like to acknowledge N. Esser, F. Flores, and G. P. Srivastava for sending us manuscripts prior to their publication. This work was supported by the Volkswagen Foundation under Grant No. I/66 407.

[1] R. M. Feenstra and P. Mårtensson, Phys. Rev. Lett. **61**, 447 (1988).

[2] R. M. Feenstra, P. Mårtensson, and J. A. Stroscio, in *Metallization and Metal-Semiconductor Interfaces,* edited by I. P. Batra (Plenum, New York, 1989), p. 307; R. M. Feenstra, P. Mårtensson, and R. Ludeke, in *Characterization of the Structure and Chemistry of Defects in Materials,* edited by B. C. Larson, M. Rühle, and D. N. Seidman, Materials Research Symposium Proceedings No. 138 (Materials Research Society, Pittsburgh, 1989), p. 305.

[3] P. Mårtensson and R. M. Feenstra, Phys. Rev. B **39**, 7744 (1989).

[4] J. Carelli and A. Kahn, Surf. Sci. **116**, 380 (1982).

[5] F. Schäffler, R. Ludeke, A. Taleb-Ibrahimi, G. Hughes, and D. Rieger, Phys. Rev. B **36**, 1328 (1987); J. Vac. Sci. Technol. B **5**, 1048 (1987).

[6] C. B. Duke, A. Paton, W. K. Ford, A. Kahn, and J. Carelli, Phys. Rev. B **26**, 803 (1982).

[7] W. K. Ford, T. Guo, D. L. Lessor, and C. B. Duke, Phys. Rev. B **42**, 8952 (1990).

[8] T. Kendelewicz, J. C. Woicik, K. E. Miyano, A. Herrera-Gomez, P. L. Cowan, B. A. Karlin, C. E. Bouldin, P. Pianetta, and W. E. Spicer, Phys. Rev. B **46**, 7276 (1992).

[9] C. A. Swarts, W. A. Goddard, and T. C. McGill, J. Vac. Sci. Technol. **17**, 982 (1982).

[10] P. Skeath, C. Y. Su, I. Lindau, and W. E. Spicer, J. Vac. Sci. Technol. **17**, 874 (1980).

[11] P. Skeath, I. Lindau, C. Y. Su, and W. E. Spicer, J. Vac. Sci. Technol. **19**, 556 (1981).

[12] P. Skeath, C. Y. Su, W. A. Harrison, I. Lindau, and W. E. Spicer, Phys. Rev. B **27**, 6246 (1983).

[13] J. P. LaFemina, C. B. Duke, and C. Mailhiot, J. Vac. Sci. Technol. B **8**, 888 (1990).

[14] C. Mailhiot, C. B. Duke, and D. J. Chadi, Phys. Rev. Lett. **23**, 2114 (1984).

[15] C. Mailhiot, C. B. Duke, and D. J. Chadi, Phys. Rev. B **31**, 2213 (1985); J. Vac. Sci. Technol. A **3**, 915 (1985).

[16] J. E. Northrup, Phys. Rev. B **44**, 1349 (1991).

[17] G. P. Srivastava, Phys. Rev. B **46**, 7300 (1992); **47**, 16 616 (1993).

[18] W. G. Schmidt, B. Wenzien, and F. Bechstedt, Verh. Dtsch. Phys. Ges. **17A**, 1506 (1993); in *Proceedings of the 4th International Conference on the Formation of Semiconductor Interfaces,* edited by J. Pollmann (World Scientific, Singapore, 1993); Czech. J. Phys. **43**, 1003 (1993).

F. J. Garcia-Vidal (unpublished); in *Proceedings of the 4th International Conference on the Formation of Semiconductor Interfaces* (Ref. 18).

[20]C. K. Shih, R. M. Feenstra, and P. Mårtensson, J. Vac. Sci. Technol. A **8**, 3379 (1990).

[21]A. Tulke, M. Mattern-Klosson, and H. Lüth, Solid State Commun. **59**, 303 (1986).

[22]A. Tulke and H. Lüth, Surf. Sci. **178**, 131 (1986).

[23]P. Mårtensson, G. V. Hansson, M. Lähdeniemi, K. O. Magnusson, S. Wiklund, and J. M. Nicholls, Phys. Rev. B **33**, 7399 (1986).

[24]W. Drube and F. J. Himpsel, Phys. Rev. B **37**, 855 (1988); F. J. Himpsel, W. Drube, A. B. McLean, and A. Santoni, Appl. Surf. Sci. **56-58**, 160 (1992).

[25]C. M. Bertoni, C. Calandra, F. Manghi, and E. Molinari, Phys. Rev. B **27**, 1251 (1983).

[26]M. Mattern-Klosson and H. Lüth, Solid State Commun. **56**, 1001 (1985).

[27]M. Mattern-Klosson, R. Strümpler, and H. Lüth, Phys. Rev. B **33**, 2559 (1986).

[28]K. Li and A. Kahn, J. Vac. Sci. Technol. A **4**, 958 (1986).

[29]W. Pletschen, N. Esser, H. Münder, D. Zahn, J. Guerts, and W. Richter, Surf. Sci. **178**, 140 (1986).

[30]W. Richter, N. Esser, A. Kelnberger, and M. Köpp, Solid State Commun. **84**, 165 (1992); N. Esser, M. Köpp, P. Haier, A. Kelnberger, and W. Richter (unpublished).

[31]R. Cao, K. Miyano, T. Kendelewicz, I. Lindau, and W. E. Spicer, Surf. Sci. **206**, 413 (1988).

[32]C. Mariani, M. G. Betti, and U. del Pennino, Phys. Rev. B **40**, 8095 (1989).

[33]G. Annovi, M. G. Betti, U. del Pennino, and C. Mariani, Phys. Rev. B **41**, 11 978 (1990); Vaccum **41**, 695 (1990).

[34]M. G. Betti, M. Pedio, U. del Pennino, and C. Mariani, Phys. Rev. B **45**, 14 057 (1992).

[35]C. Goletti, P. Chiaradia, W. Jian, and G. Chiarotti, Solid State Commun. **84**, 421 (1992).

[36]P. Hohenberg and W. Kohn, Phys. Rev. **136**, 864 (1964).

[37]W. Kohn and L. J. Sham, Phys. Rev. **140**, 1133 (1965).

[38]L. Kleinman and D. M. Bylander, Phys. Rev. Lett. **48**, 1425 (1982).

[39]R. Stumpf, X. Gonze, and M. Scheffler (unpublished); X. Gonze, R. Stumpf, and M. Scheffler, Phys. Rev. B **44**, 8503 (1991).

[40]D. R. Hamann, M. Schlüter, and C. Chiang, Phys. Rev. Lett. **43**, 1494 (1979).

[41]G. B. Bachelet, D. R. Hamann, and M. Schlüter, Phys. Rev. B **26**, 4199 (1982).

[42]D. M. Ceperley and B. I. Alder, Phys. Rev. Lett. **45**, 566 (1980).

[43]P. Perdew and A. Zunger, Phys. Rev. B **23**, 5048 (1981).

[44]M. Schlüter, J. R. Chelikowsky, S. G. Louie, and M. L. Cohen, Phys. Rev. B **12**, 4220 (1975).

[45]R. A. Evarestov and V. P. Smirnov, Phys. Status Solidi B **119**, 9 (1983).

[46]R. Car and M. Parrinello, Phys. Rev. Lett. **55**, 2471 (1985).

[47]R. Stumpf and M. Scheffler, Comput. Phys. Commun. (to be published).

[48]W. A. Harrison, *Electronic Structure and the Properties of Solids* (Dover, New York, 1989).

[49]B. Farid and R. J. Needs, Phys. Rev. B **45**, 1067 (1992).

[50]J. Hebenstreit, Adv. Solid State Phys. **31**, 165 (1991).

[51]*Table of Periodic Properties of the Elements* (Sargent-Welch Sci. Comp., Skokie, IL, 1980).

[52]J. L. Alves, J. Hebenstreit, and M. Scheffler, Phys. Rev. B **44**, 6188 (1991).

[53]F. Bechstedt and M. Scheffler, Surf. Sci. Rep. **18**, 145 (1993).

[54]F. Bechstedt and R. Del Sole, Solid State Commun. **74**, 41 (1990).

[55]F. Bechstedt, Adv. Solid State Phys. **32**, 161 (1992).

[56]J. Hebenstreit, M. Heinemann, and M. Scheffler, Phys. Rev. Lett. **67**, 1031 (1991); J. Hebenstreit and M. Scheffler, Phys. Rev. B **46**, 16 134 (1992).

[57]A. I. Shkrebtii, R. Del Sole, P. Chiaradia, C. Goletti, and Wang Jian, in *Proceedings of the 4th International Conference on the Formation of Semiconductor Interfaces* (Ref. 18).

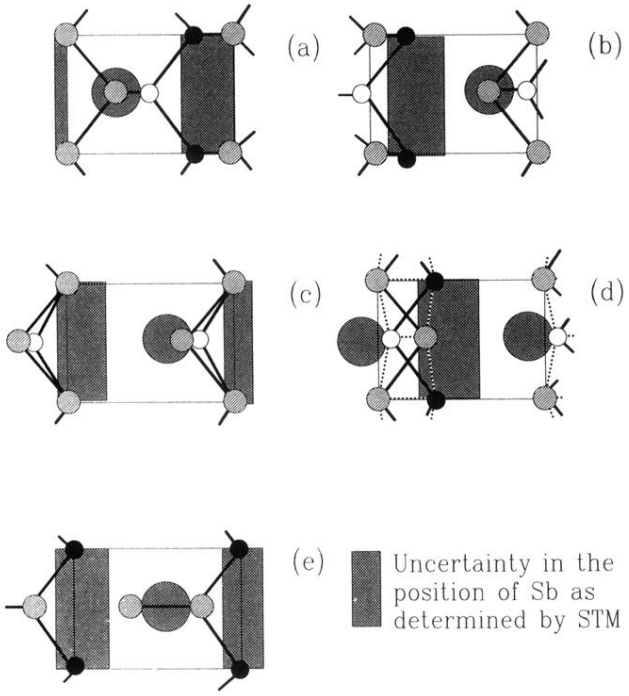

FIG. 3. Comparison of the spatial locations of the topographic features observed in the STM images by Mårtensson and Fenstra[3] with the fully relaxed positions derived by total-energy minimization for different structural models: (a) ECLS, (b) p^3 structure, (c) EOTS, (d) EOCS, and (e) dimer model.